



48 distinguishes between the upper or anomalous dataset from lower or background datasets (Sinclair  
49 1974). Determination of threshold values have been carried out for different types of geoscience related  
50 datasets ranging from geochemical, geophysical, remote sensing and environmental studies using a  
51 variety of statistical techniques. (Sinclair, 1987; Aramesh *et al.*, 2013, Chang, 1997). This study is  
52 aimed at inventing a new method for defining thresholds from spatial profiles in thematic images.  
53 Spatial profiling method for threshold determination is targeted towards determining maximum and  
54 minimum threshold values by constructing profiles across very high and very low altered zones.

### 56 **REGIONAL GEOLOGY OF THE STUDY AREA:**

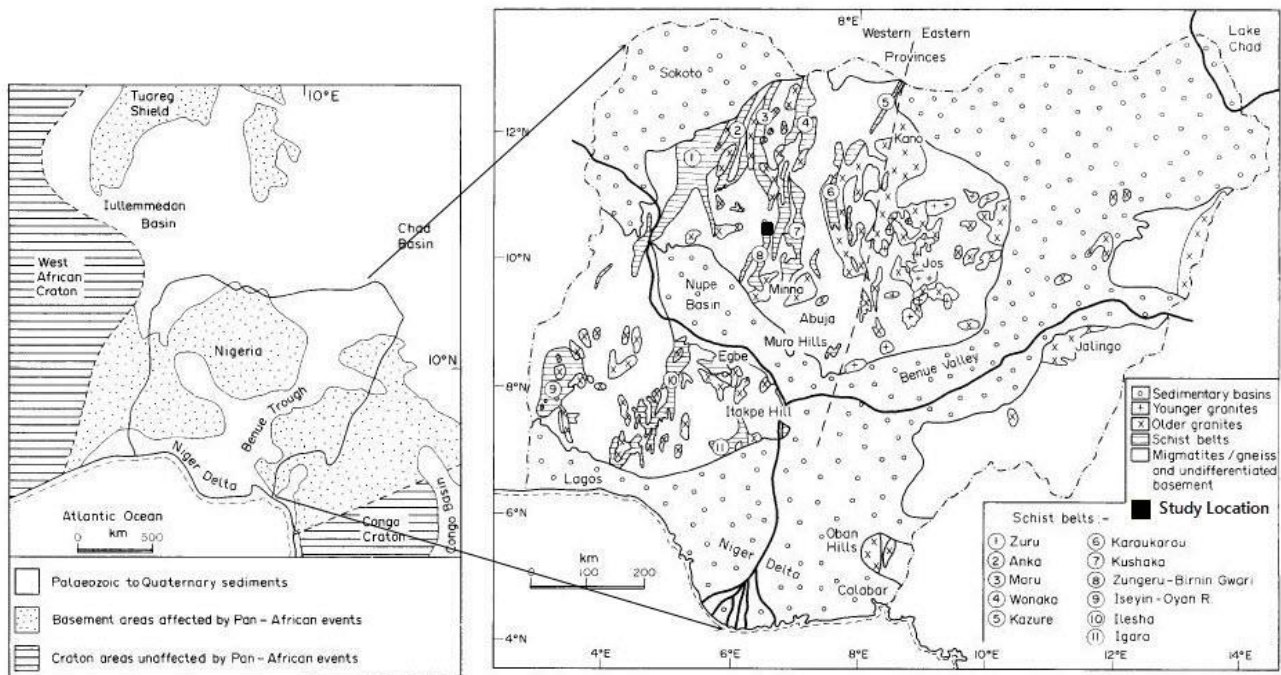
57  
58  
59  
60 The study area is situated within the latitudes 10° 33' 32.7" to 10° 39' 50" and longitudes 6° 38' 38" to  
61 6° 43' 40" (Fig. 1). According to Black (1980), it is located within the Nigerian Basement Complex  
62 which form parts of the Pan African mobile belts. It occupies the reactivated region that results from  
63 plate collision between the passive continental margin of the West African craton and the active  
64 Pharusian continental margin affected by the Pan African Orogeny (Burke and Dewey; 1972, Dada  
65 2006). Lithologically, the Nigerian Basement Complex can be sub divided into Migmatite Gneiss  
66 Complex (MGC), the Older Metasediments, the Younger Metasediments and the Older Granites. The  
67 Migmatitic gneiss complex is the oldest rock units of the Basement Complex, it is dated as Birrimian  
68 in age (about 250 Ma). It is believed to be of sedimentary origin but was later profoundly altered into  
69 metamorphic and granitic conditions (McCurry 1970, 1976). It comprises of Archean polycyclic grey  
70 gneiss of granodiorite to tonalitic composition and it is considered to be the Basement *Sensu Stricto*  
71 (Rahaman 1988, Dada 2006).

73  
74 The Older meta-sediments are among the earliest rocks form on the Nigerian Basement Complex.  
75 Initially of sedimentary origin with a more extensive distribution. The Older meta-sediments have  
76 undergone prolonged, repeated metamorphism and now occurs as quartzites (ancient sandstones),  
77 mudrock (ancient claystones) and other calcareous relics of highly altered clay sediments and igneous

78 rocks. The Younger Metasediments are late pelites (represented by phyllites, muscovites schists and  
 79 biotite schists) with quartzites forming the dominant ridge in several in most of the belts. Some belts  
 80 contain ferruginous and banded quartzites, spassetite-bearing quartzites, conglomerates, horizon  
 81 marbles and calc-silicates.

82  
 83 The Older Granites of Nigeria are widely spread throughout the basement complex and occurs as large  
 84 circular masses. They consist of a wide spectrum of rocks which vary in composition from tonalite  
 85 through granodiorite to granite, syenite and charnokitic rocks (Trustwell *et al.*, 1963). The granitoids  
 86 have been emplaced into both the migmatite-gneiss complex and the schist belts. The north-south  
 87 linear aggregation of many large batholiths within the Basement Complex suggests that they may be  
 88 related to deep-seated pre-existing plutonic episodes controlled by deep mantle structures (Ogezi,  
 89 1977).

90  
 91



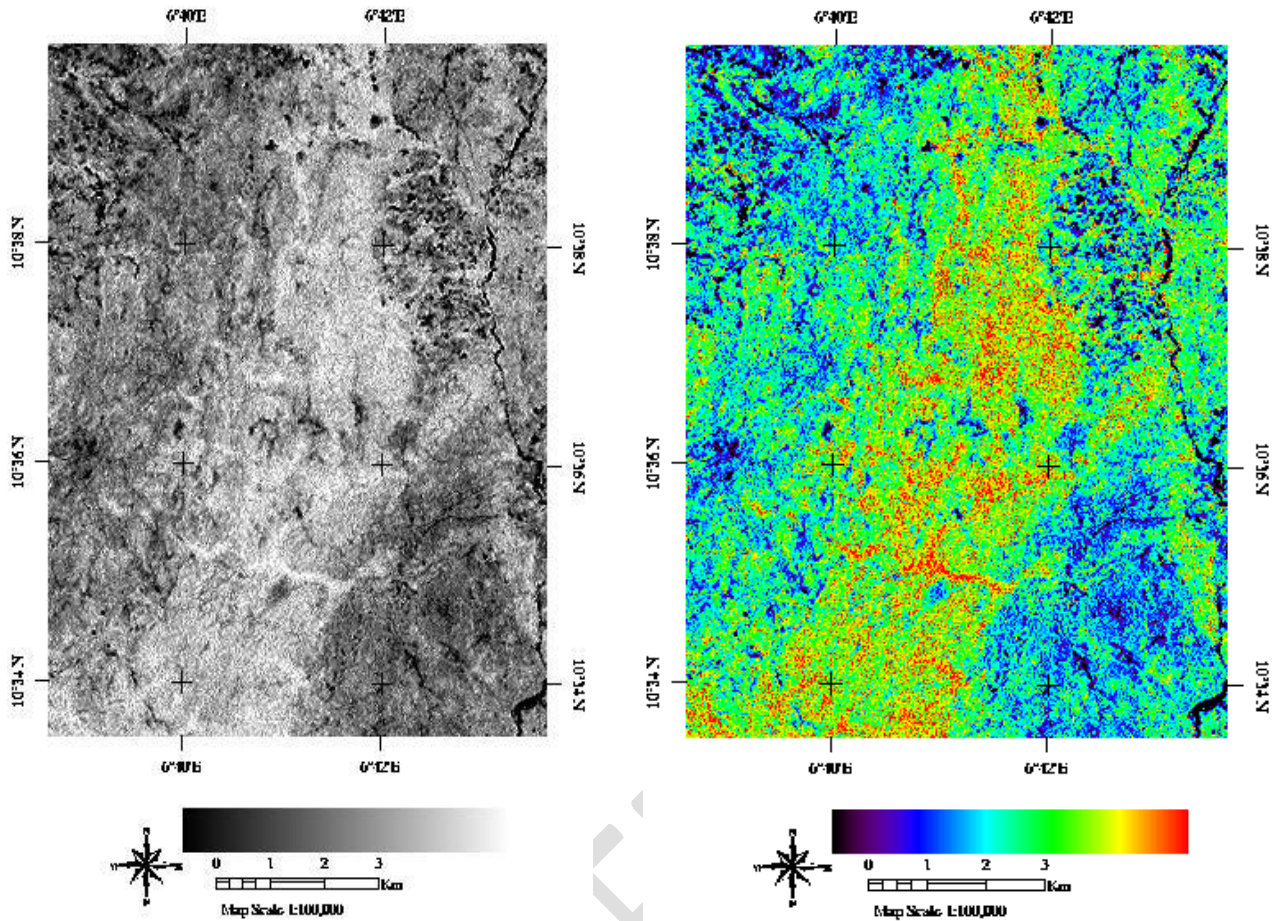
92  
 93  
 94

Figure 1: Regional Geology of the Study area (Modified after *et.al* 1987)

95 **METHODS:**

96 **Band Ratio**

97 This is an image processing method where digital numbers (brightness values) of one band is divided  
98 by that of another band. It corresponds to the peak of high and low reflectance curves (Pour and  
99 Hashim, 2015). The technique improves the contrast and enhances compositional information while  
100 suppressing less useful information like earth's surface and topographic shadow, thus highlighting  
101 some features that cannot be seen in raw data (Sabins, 1999; Vander Meer, 2004; Ali and Pour, 2014).  
102 Since gold mineralization within the study area is associated with clay alterations, a band ratio image  
103 5/7 was generated to show the intensity of the clay alterations from dark to white. The dark colour  
104 represents low clay alteration while the white represents high clay alterations (Fig. 2A). For better  
105 display, ENVI 4.5 color tool was used to display these variations in clay alteration intensity from blue  
106 which represents low to red which represents high zones (Figure, 2B).



108  
109  
110

**Figure 2: Band ratio image 5/7 displaying clay alterations A = Black and white image  
B = Colour image.**

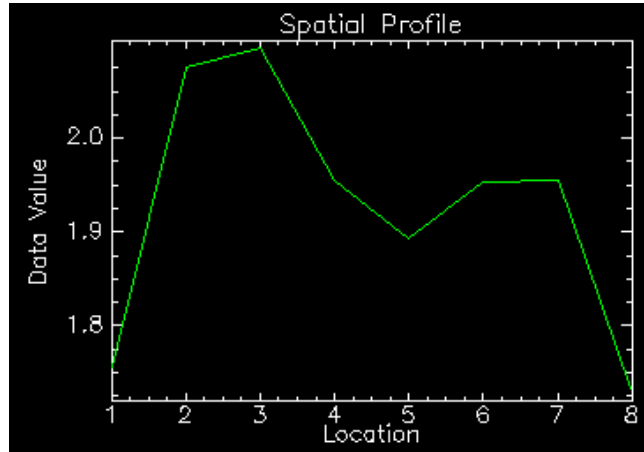
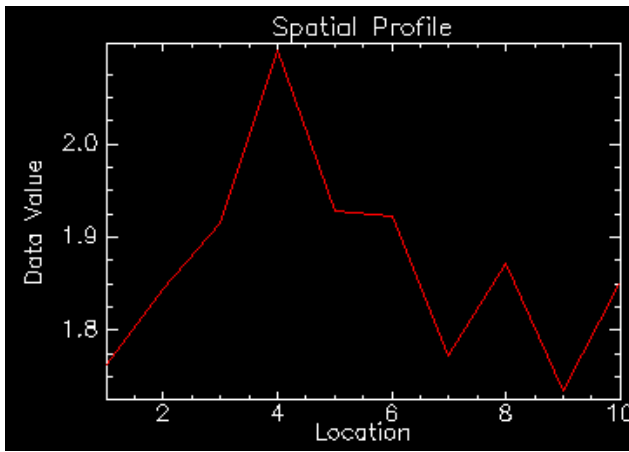
111 **Threshold Mapping:**

112 Threshold mapping involves finding that value which separates regions of high and low alteration  
113 from background. In this study, 10 profiles each were constructed from anomalous high and low altered  
114 zones.

115 **Maximum Threshold Mapping**

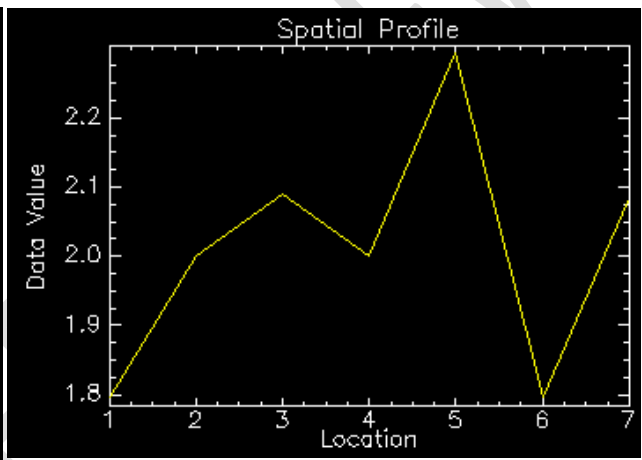
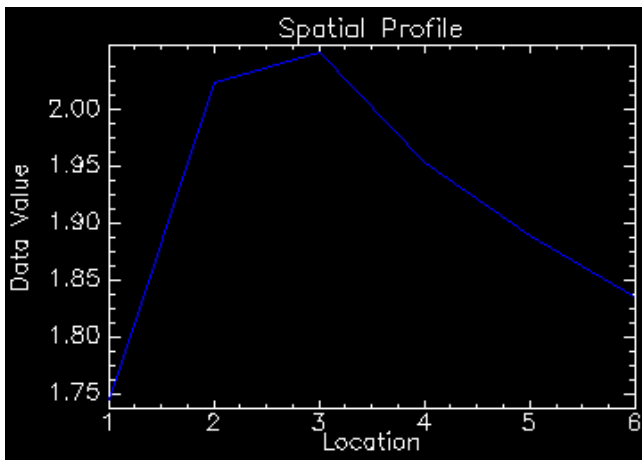
116 For determining the maximum threshold value, 10 micro profiles were constructed across highly  
117 altered zones within the study area (Figure 3). From these profiles, the maximum reflectance value for  
118 all the 10 profiles were extracted, summed and the mean calculated (Table 1). The mean value was  
119 assumed to be the maximum threshold value. The maximum threshold value was then used to  
120 segregate and delineate highly altered areas within the study location (Figure 4).  
121

122



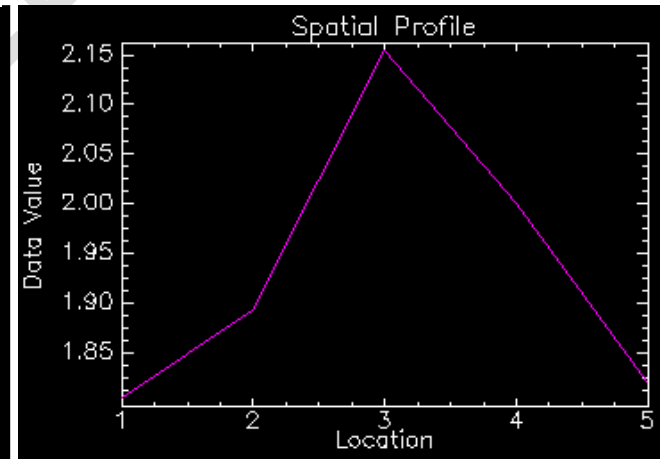
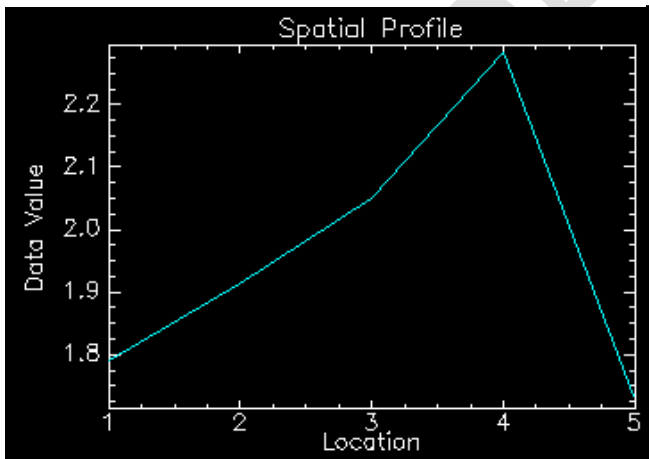
123

124



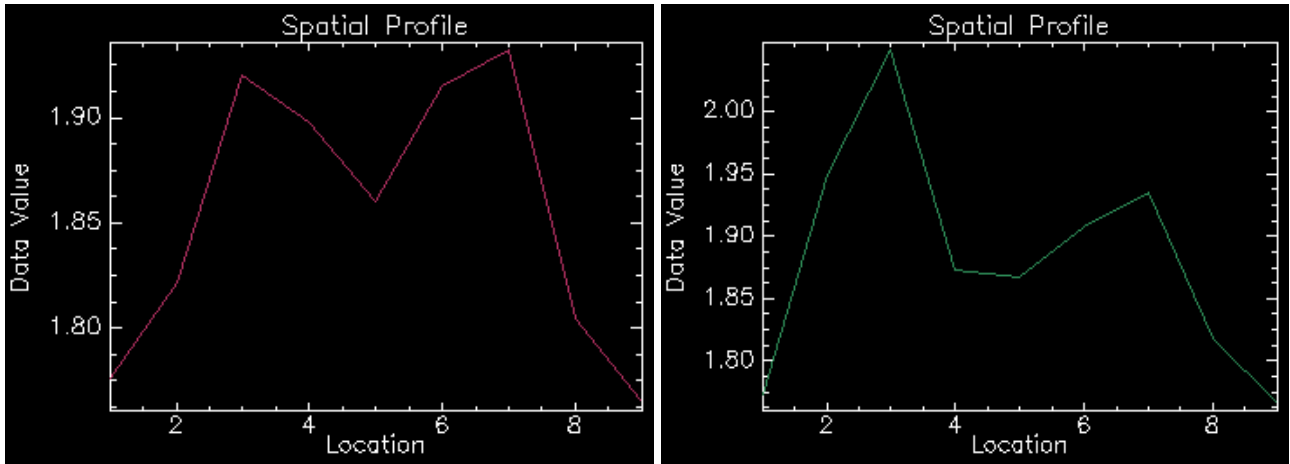
125

126

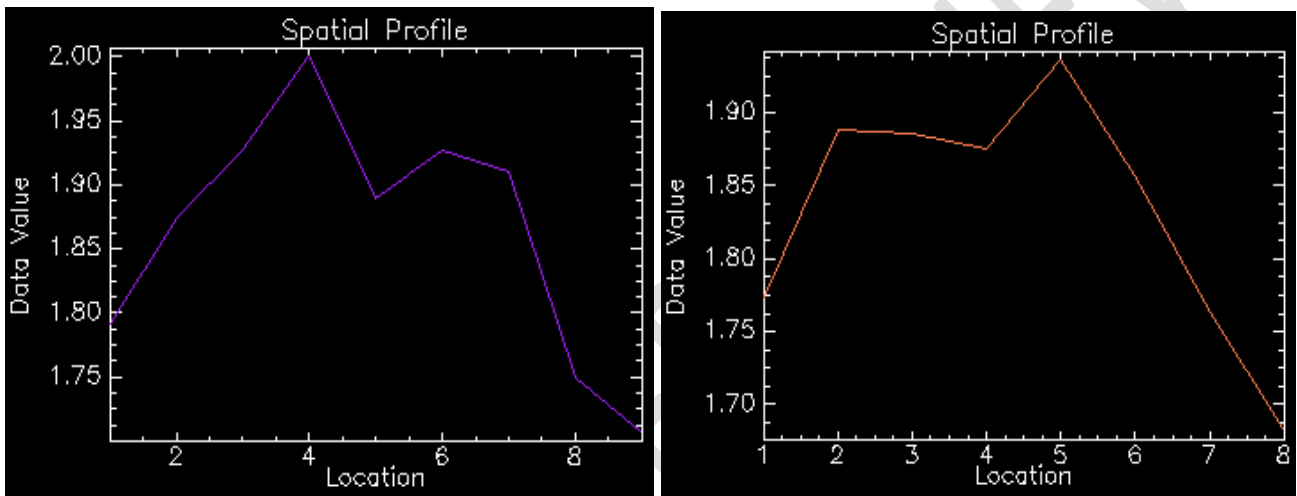


127

128



129  
130

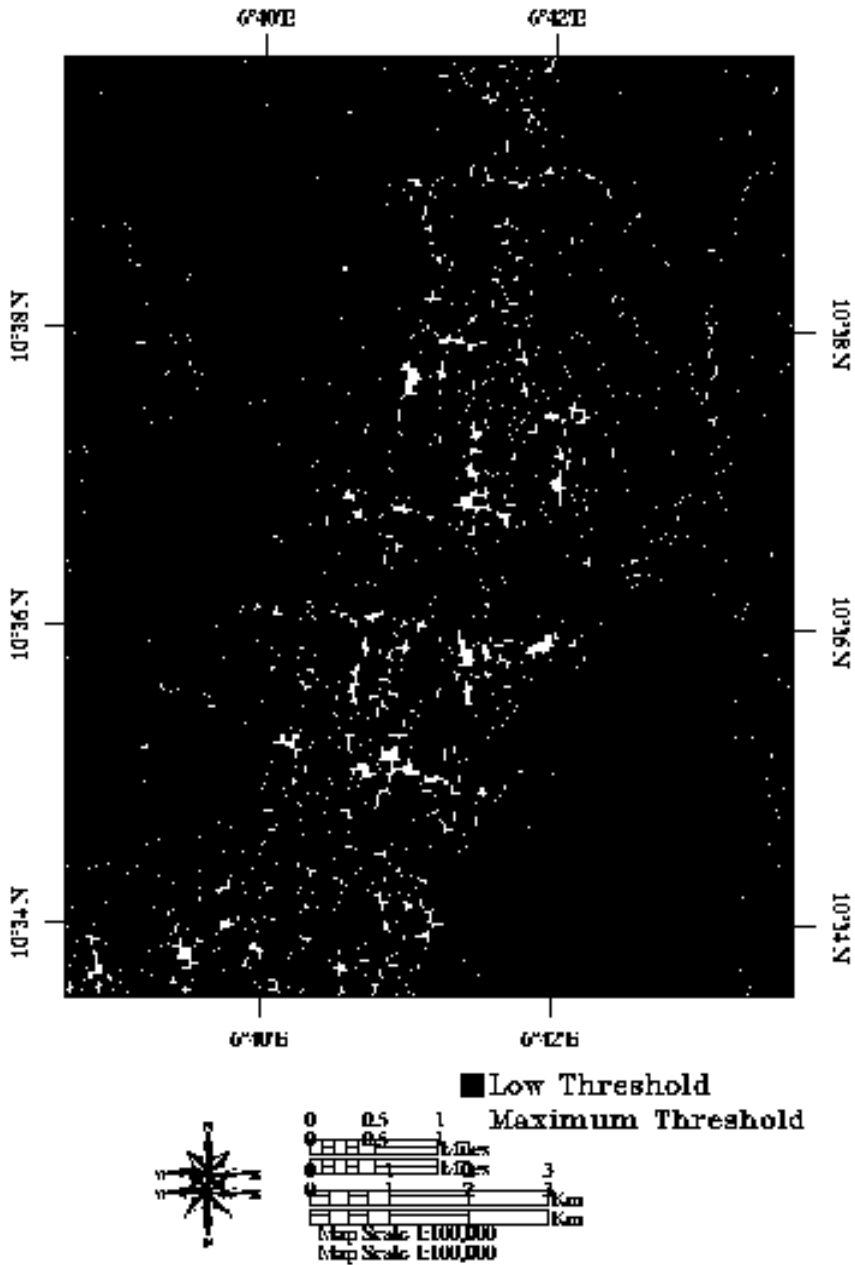


131  
132

133 Figure 3: Spectral Profiles across high anomalous zones within the study area

134

135 Segregation using threshold values were carried out with a decision tree algorithm of ENVI 4.5  
136 software. After the segregation, clump class function was applied to enhance highly anomalous zones  
137 within the study area (Figure 4).

139  
140

141 Figure 4: High threshold zones for the study area

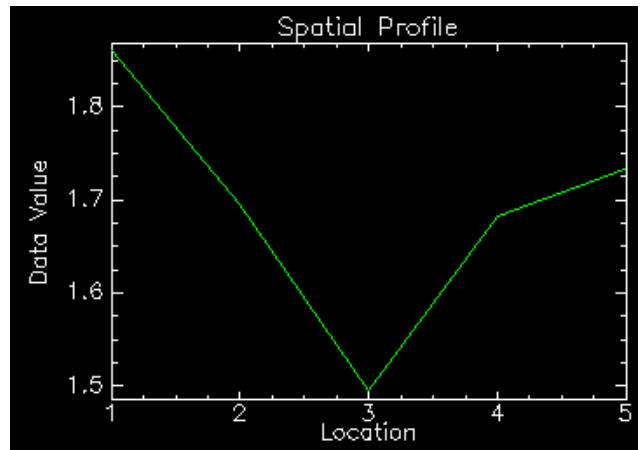
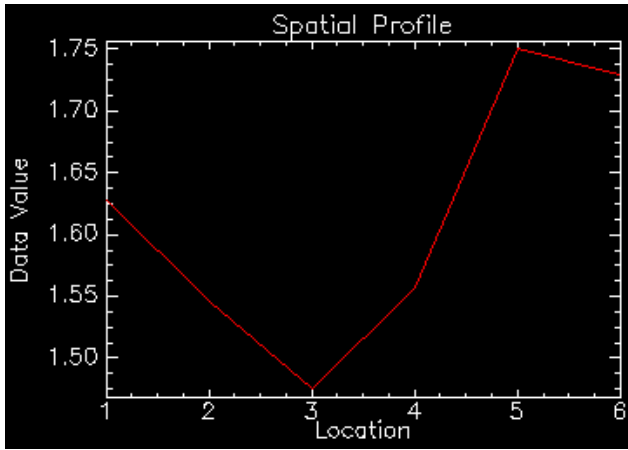
142

143 **Minimum Threshold Mapping**

144

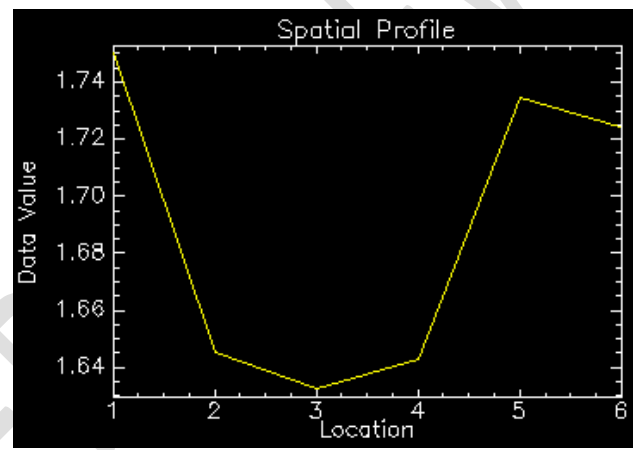
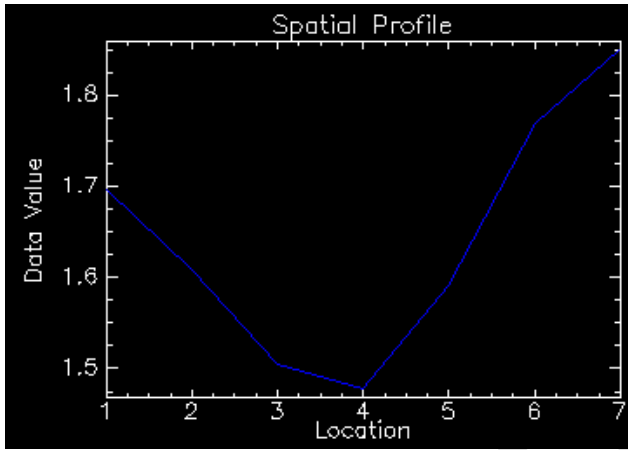
145 In determining the minimum threshold value, 10 micro profiles were constructed across very low  
 146 anomalous zones (Figure 4). From this profiles, the minimum reflectance value were extracted,  
 147 summed and the mean determined. The mean was assumed to be the minimum threshold (Table 1).

148



149

150

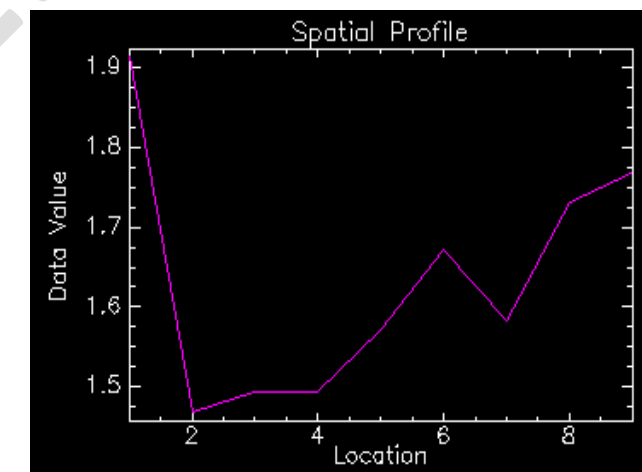
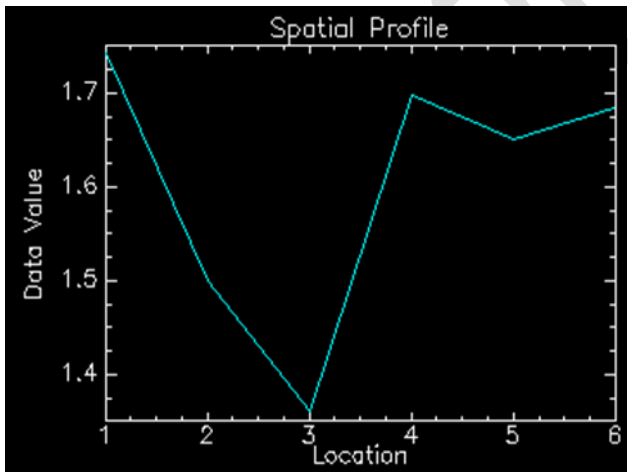


151

152

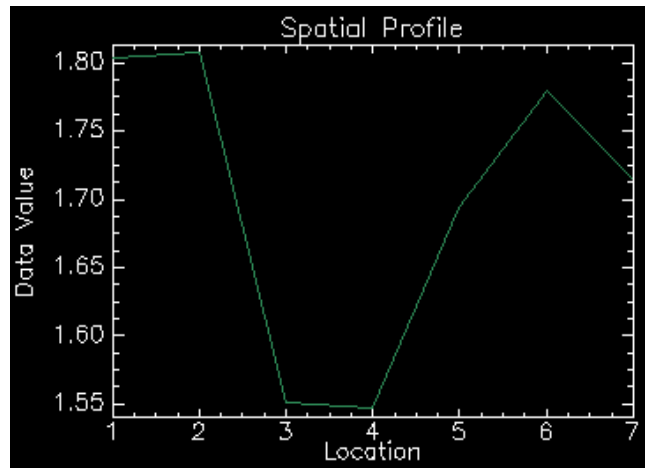
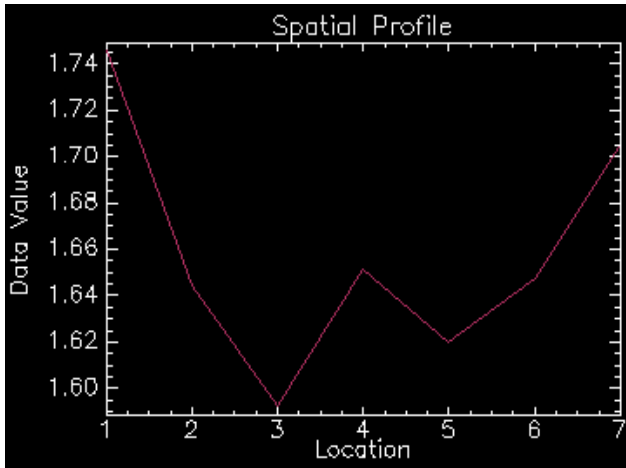
153

154

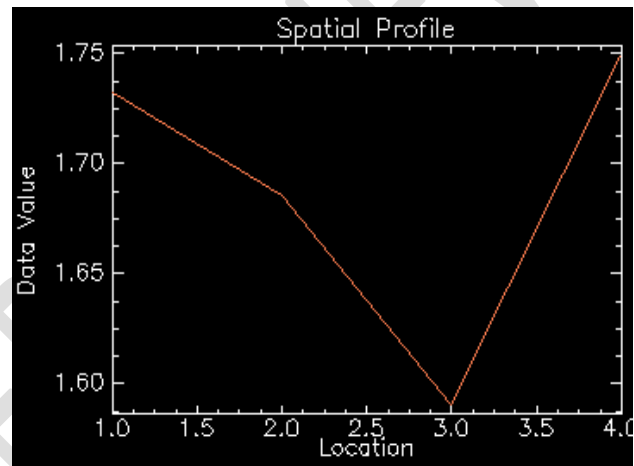
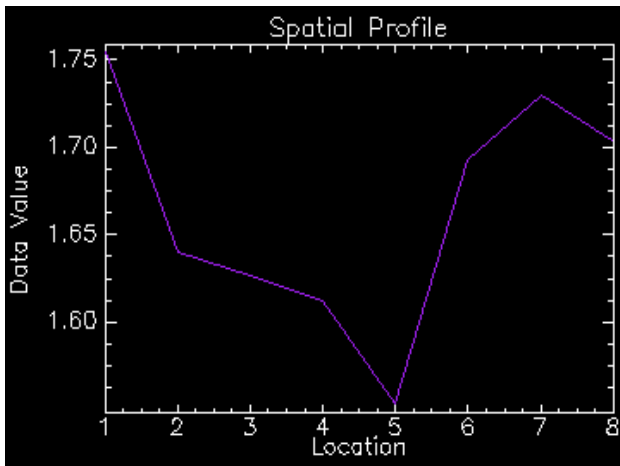


155

156



157  
158



159  
160

Figure 5: Spectral profile across low anomalous zones within the study area

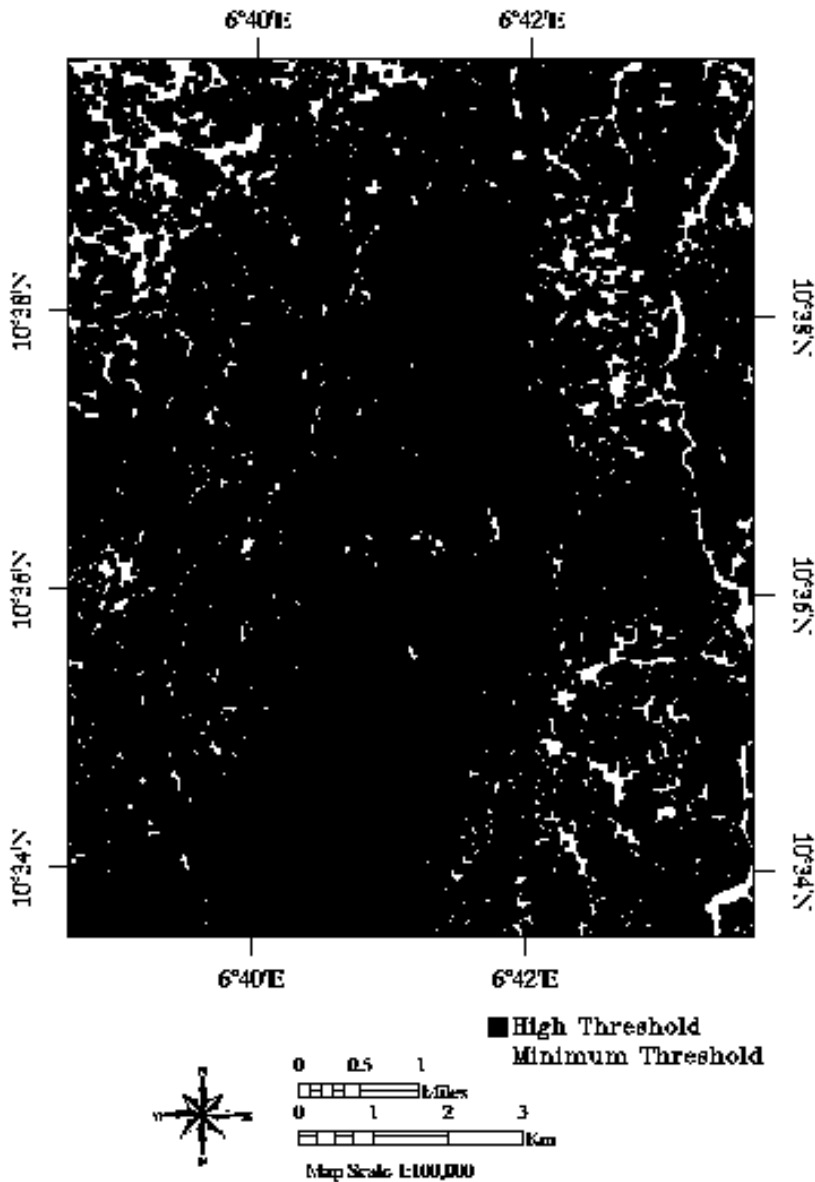
161  
162

The minimum threshold value was used to segregate zones of low alteration within the study area using decision tree algorithm in ENVI 4.5 software. Clump class function was also applied to enhance low alteration zones (Figure 6).

166  
167  
168  
169

Table 1: Threshold statistics for altered imagery along profiles

	P1	P 2	P 3	P4	P 5	P 6	P7	P8	P9	P10	Total	Threshold
Max	2.1	2.09	2.05	2.29	2.28	2.15	1.932	1.95	2	1.94	20.782	2.078
Min	1.55	1.5	1.48	1.63	1.36	1.47	1.59	1.55	1.55	1.59	15.27	1.527



171

172

173 Figure 5: Low threshold zones within the study area

174

175 **Validation of Threshold Method**

176

177

178 The validation of spatial profiling method for calculating threshold values for any geodata set were  
 179 carried out by comparing threshold values obtained from spatial profiling method to threshold values  
 180 computed using other established methods. For convinence, the spatial profiling threshold values were  
 compared to the mathematical method for calculating the threshold as stated below.

181

$$\text{Maximum Threshold} = \text{Mean} + 2 * \text{Standard deviation}$$

182

$$\text{Minimun Threshold} = \text{Mean} - 2 * \text{Standard deviation}$$

183

184

185

The comparison of threshold values from both methods are presented in Table 2.

186 **Table 2: Threshold validation for spatial profiling**

S/N	Threshold	Method	Value
1	Maximum Threshold	Maximum Spatial Profiling	2.078
		Mean + 2* Standard deviation	2.06
2	Minimum Threshold	Minimum Spatial Profiling	1.527
		Mean – 2* Standard Deviation	1.5

187  
188  
189

190 **Implications of spatial profiling technique for Mineral exploration**

191  
192 Mineral exploration deals with the search for mineralisation within a particular area. Thus Remote  
193 sensing technique is highly valuable in exploration programs because of its ability to map not just  
194 alterations types associated with mineralisation but also the degree of alteration. Therefore the higher  
195 and the degree of alteration the greater the chances of finding a mineral deposit. Mapping the degree  
196 of alteration is possible by defining threshold values and using these values for segregating delineating  
197 areas of low, moderate and high alterations. Before carrying out such a task, the knowledge of  
198 alterations associated with mineralisation in these areas must be known. This study has proven that  
199 gold mineralisation is associated with clay alteration. Further more, clay alteration from satellite  
200 imagery was quantified using threshold values derived from spatial profiling method. Known zones  
201 of gold mineralisation were plotted to establish relationship between clay alteration and gold  
202 mineralisation.

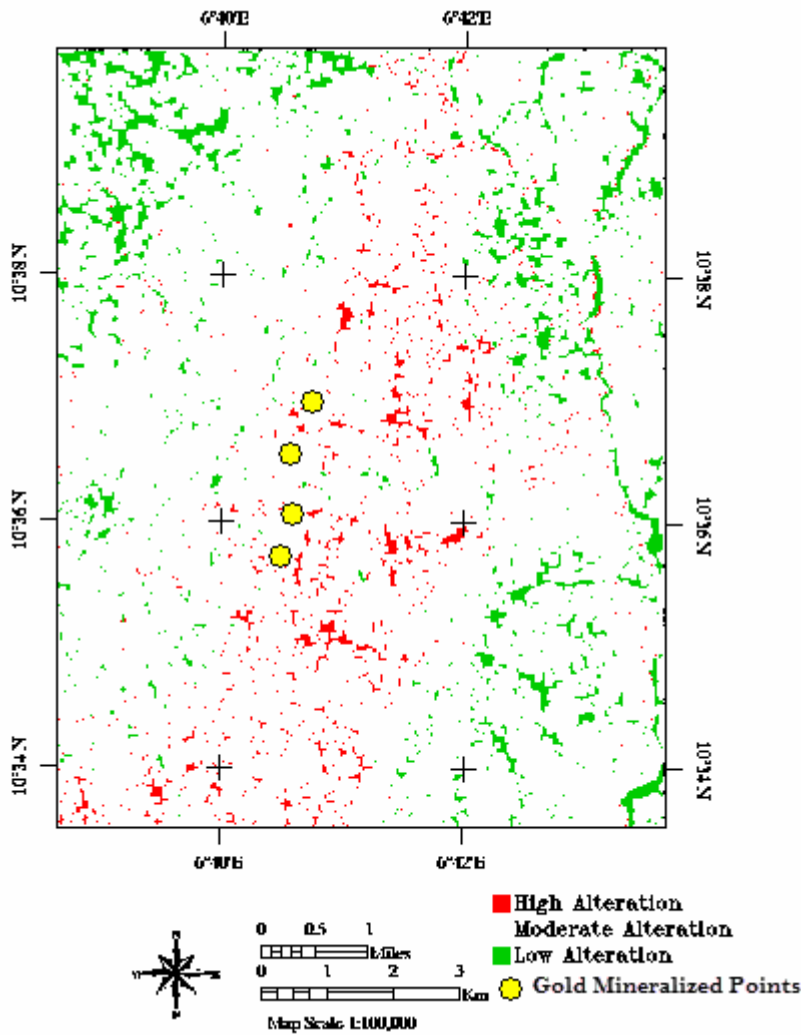
204  
205

Figure 6: Relationship between gold mineralisation and alterations within the study area

207  
208

## RESULT AND DISCUSSION

209  
210

The use of remote sensing in mapping mineral deposits associated with alteration becomes easier when threshold values are defined and used to segregate highly altered zones from low altered zones. The rationale behind this method relies on the fact that mineralisation tend to increase with the degree of alteration. From this study, it was observed that the spatial profile method is an alternative method for defining and quantifying geo-data set within any thematic layer of interest. This is evident from the close similarities of threshold values computed from standard techniques to those obtained using spartial profile method. Applying the computed values to a well processed band ratio imagery was able to define regions of low and high alteration within the study area. The resulting imagery revealed that the highly altered zones dominates the central part of the study area along a N-S trend and it is being

218

219 flanked by a low altered zone. Zones of intermediate alterations are peppered throughout the study  
220 area. Well known zones of gold mineralisation within the study area all plotted within the highly  
221 altered zones confirming location of gold mineralisation within the highly altered zones.

## 222 CONCLUSION

223 The spatial profile method for defining threshold values in any geoscience dataset is valid and  
224 effective especially for data displayed in thematic layer format. Application of this method for  
225 mapping hydrothermal alteration have proved to be very effective in defining zones of high alterations  
226 within the study area. A close correlation has been shown to exist between highly altered zones and  
227 known mineralisation points within the study area. Spatially, the highly altered zones assumed a  
228 general N-S trend within the central part of the study area. Therefore the higher and the degree of  
229 alteration the greater the chances of finding a mineral deposit. Mapping the degree of alteration is  
230 possible by defining threshold values and using these values for segregating delineating areas of low,  
231 moderate and high alterations. The study established that known gold mineralization points in the study  
232 area were observed to occur within the highly altered clay alteration zones.

## 236 REFERERENCES

- 233  
234  
235  
236  
237  
238 Ali, A., & Pour, A., (2014). Lithological mapping and hydrothermal alteration using Landsat 8 data: a  
239 case study in ariab mining district, red sea hills, Sudan. *International Journal of Basic and Applied*  
240 *Sciences*, 3(3), 199–208.  
241  
242 Aramesh A.R, Afzal P., Adib A., Yasrebi B.A (2014) Application of multi fractal modelling for  
243 identification of alteration zones and major faults based on ETM+ multispectral data. *Arabian Journal*  
244 *of geoscience* 10.1007/s12517-01401366-2.  
245  
246 Black R (1980) Precambrian of West Africa. Episodes 4:3–8  
247  
248 Burke, K.C. and Dewey, J.F. (1972). Orogeny in Africa. In: Dessauvage TFJ, Whiteman AJ (eds),  
249 Africa geology. *University of Ibadan Press*, Ibadan, pages 583–608.  
250  
251 Cheng, Q., (1994). Multifractal Modeling and Spatial Analysis with GIS: Gold Mineral Potential  
252 Estimation in the Mitchell-Sulphurets Area, Northwestern British Columbia, Ph.D. Thesis, University  
253 of Ottawa, Ottawa, 268 pp.

- 254 Dada, S.S. (2006). Proterozoic evolution of Nigeria. In: Oshi O (ed) The basement complex of Nigeria  
255 and its mineral resources (A Tribute to Prof. M. A. O. Rahaman). *Akin Jinad and Company Ibadan*,  
256 pages 29–44.
- 257  
258 Mc Curry (1970). The geology of degree sheet 21 (Zaria) (M.Sc thesis) Zaria, Nigeria, Ahmadu Bello  
259 University, 139p.
- 260  
261 McCurry, P. (1976). The geology of the Precambrian to Lower Palaeozoic Rocks of Northern Nigeria  
262 – A Review. In: Kogbe CA (ed) *Geology of Nigeria. Elizabethan Publishers, Lagos*, pages 15–39.  
263  
264
- 265 Ogezi, A.E.O. (1977). Geochemistry and Geochronology of Basement Rocks from Northwestern  
266 Nigeria. Unpublished Ph.D. Thesis, University of Leeds.  
267  
268
- 269 Pour, A., & Hashim, M., (2015). Hydrothermal alteration mapping from Landsat-8 data, Sar Chesmeh  
270 copper mining district, south-eastern Islamic Republic of Iran. *Journal of Taibah University for  
271 Science*, 9, 155-166.  
272
- 273 Rahaman, M.A. (1988). Recent advances in the study of the basement complex of Nigeria. In:  
274 *Geological Survey of Nigeria (ed) Precambrian Geology of Nigeria*, pages 11–43.  
275
- 276 Sabins, F.F., (1997). Remote Sensing — Principles and Interpretation, 3rd edn., W.H. Freeman, New  
277 York, NY., 494 pp.  
278
- 279 Sabins, F.F., (1999). Remote sensing for mineral exploration. *Ore Geology Reviews* 14, 157–183.
- 280 Sinclair AJ. (1974) Selection of threshold values in geochemical data using probability graphs. *J*  
281 *Geochem Explor* 3:129 – 49.  
282
- 283 Truswell, J.F. and Cope, R.N. (1963). The geology of parts of Niger and Zaria Provinces, Northern  
284 Nigeria. *Geol Suvey Nigeria Bull* 29:1–104.  
285
- 286 Van der Meer, D. F. (2004). Analysis of spectral absorption features in hyperspectral imagery.  
287 *International Journal of Applied Earth Observation and Geoinformation*, 5, 55 – 68.  
288
- 289 Woakes M., Rahaman M.A., Ajibade A.C., (1987). Some Metallogenic Features of the Nigerian  
290 Basement. *Journal of African Earth Sciences*, Vol. 6, No 5, pp 655-664.